HHS Public Access

Author manuscript

Science. Author manuscript; available in PMC 2022 February 10.

Published in final edited form as:

Science. 2021 June 04; 372(6546): 1068–1073. doi:10.1126/science.abg1774.

Reciprocal repulsions instruct the precise assembly of parallel hippocampal networks

Daniel T. Pederick[1], **Jan H. Lui**[1], **Ellen C. Gingrich**[1,2], **Chuanyun Xu**[1], **Mark J. Wagner**[1], **Yuanyuan Liu**[3,†], **Zhigang He**[3], **Stephen R. Quake**[4,5], **Liqun Luo**[1,*]

[1]Department of Biology, Howard Hughes Medical Institute, Stanford University, Stanford, CA, USA

[2]Neurosciences Graduate Program, Stanford University, Stanford, CA, USA

[3]F.M. Kirby Neurobiology Center, Department of Neurology, Boston Children's Hospital, Harvard Medical School, Boston, MA, USA

[4]Departments of Bioengineering and Applied Physics, Stanford University, Stanford, CA, USA

[5]Chan Zuckerberg Biohub, Stanford, CA, USA

Abstract

Mammalian medial and lateral hippocampal networks preferentially process spatial- and object-related information, respectively. However, the mechanisms underlying the assembly of such parallel networks during development remain largely unknown. Here, we show that, in mice, complementary expression of cell-surface molecules Teneurin-3 (Ten3) and Latrophilin-2 (Lphn2) in the medial and lateral hippocampal networks, respectively, guides the precise assembly of CA1-to-subiculum connections in both networks. In the medial network, Ten3+ axons are repelled by target-derived Lphn2, revealing that Lphn2/Ten3-mediated repulsion and Ten3/Ten3-mediated attraction cooperate to control precise target selection of CA1 axons. In the lateral network, Lphn2+ CA1 axons are confined to Lphn2+ targets via repulsion from Ten3+ targets. Our findings demonstrate that assembly of parallel hippocampal networks follows a 'Ten3→Ten3, Lphn2→Lphn2' rule instructed by reciprocal repulsions.

One Sentence Summary:

Complementary expression and reciprocal repulsion of multifunctional cell-surface proteins instruct axons in search of targets as the mouse hippocampal networks develop.

*Corresponding author (lluo@stanford.edu).

†Current address: Somatosensation and Pain Unit, National Institute of Dental and Craniofacial Research (NIDCR), National Center for Complementary and Integrative Health (NCCIH), National Institutes of Health, Bethesda, MD, USA

Author contributions: D.T.P. performed all the experiments and analyzed the data, except for single-cell sequencing sample collection and data processing which was performed by J.H.L., with support from S.R.Q. E.C.G. and C.X. assisted in tissue processing. M. J. W. generated MATLAB code and analyzed data. Y.L. and Z.H. produced custom lentivirus. L.L. supervised the study. D.T.P., J.H.L., and L.L. wrote the paper.

Competing interests: The authors declare no competing interests.

Supplementary Materials:
Materials and Methods
Figures S1 to S11
Tables S1
References (27–40)

Parallel information processing is a salient feature of complex nervous systems. One example is the mammalian hippocampal-entorhinal network, essential for explicit memory formation and spatial representation (1–4). Spatial- and object-related information is preferentially processed by the medial and lateral hippocampal networks, respectively (5, 6). In the medial network, proximal CA1 axons project to distal subiculum (Fig. 1A, cyan), and both proximal CA1 and distal subiculum also form reciprocal connections with the medial entorhinal cortex. In the lateral network, distal CA1 axons project to proximal subiculum (Fig. 1A, yellow), and both distal CA1 and proximal subiculum form reciprocal connections with the lateral entorhinal cortex (7, 8) (fig. S1A).

We previously showed that the type II transmembrane protein Teneurin-3 (Ten3) has matching expression in all interconnected regions of the medial hippocampal network (9). Ten3 is required in both proximal CA1 and distal subiculum for target selection of the proximal CA1→distal subiculum axons, and promotes aggregation of non-adhesive cells (9). These data support a homophilic attraction mechanism by which Ten3 regulates target selection in the medial hippocampal network. It remains unclear whether matching gene expression exists in the lateral hippocampal network and how this contributes to parallel hippocampal network assembly.

Complementary Lphn2/Ten3 expression across parallel hippocampal networks

We hypothesized that cell-surface molecules with inverse patterns to *Ten3*, and therefore enriched in the lateral hippocampal network, may play a role in the precise assembly of parallel hippocampal networks. To identify such genes, we performed fluorescence-activated cell sorting–based single-cell RNA sequencing of postnatal day 8 (P8) excitatory neurons that express vesicular glutamate transporter 1, in subregions of the medial or lateral networks (figs. S1–2). Among cell-surface molecules differentially expressed in CA1 and subiculum (fig. S3A), we identified *Latrophilin-2* (*Lphn2*), an adhesion G-protein-coupled receptor (GPCR) known to bind Teneurins (10–15), that showed inverse expression to *Ten3* not only in CA1 and subiculum but also in entorhinal cortex (Fig. 1B; fig. S4A; table S1). Other *Teneurin* and *Latrophilin* family members did not display such differential expression (fig. S3B and C).

Double *in situ* hybridization for *Lphn2* and *Ten3* mRNA in P8 mouse brain revealed preferential expression of *Lphn2* in distal CA1, proximal subiculum, and lateral entorhinal cortex, complementary to *Ten3* enrichment in proximal CA1, distal subiculum, and medial entorhinal cortex (Fig. 1C, D; fig. S4B, C). We also examined protein expression using an anti-Ten3 antibody (9) and an anti-GFP antibody in *Lphn2-mVenus* knock-in mice (16). In all regions, Lphn2 and Ten3 proteins were expressed in the synaptic layers corresponding to their mRNA expression, including the molecular layer of CA1, the cell body and molecular layers of subiculum, and layer III of entorhinal cortex (Fig. 1E, F; fig. S4D, E). Thus, *Lphn2* and *Ten3* mRNA, as well as Lphn2 and Ten3 proteins, exhibit complementary expression in multiple regions of the developing hippocampal networks, including CA1, subiculum, and

entorhinal cortex (fig. S4F). In all cases, the connection specificity follows a 'Ten3→Ten3, Lphn2→Lphn2' rule that correlates cell-surface molecule expression with connectivity.

In the rest of this study, we focus on the target selection of CA1→subiculum axons to investigate the developmental mechanisms by which the 'Ten3→Ten3, Lphn2→Lphn2' rule is established. Ten3+ and Lphn2+ CA1 axons extend along a tract above the subiculum cell body layer until they reach Ten3+ distal subiculum and Lphn2+ proximal subiculum, respectively, where they invade the cell body layer of the subiculum to form synapses (9) (fig. S5). Lphn2 and Ten3 proteins were first detected in subiculum targets (by P2) and displayed increasing expression in CA1 in subsequent days; by P8, the highest levels of Lphn2 and Ten3 in CA1 and subiculum are comparable (fig. S6). This increase in expression coincides with the timing of target selection of CA1 axons in subiculum (9).

Subiculum Lphn2 repels Ten3+ CA1 axons

Ten3 directs axon targeting in the medial hippocampal network through matching expression and homophilic attraction (9). Does Lphn2 also mediate homophilic attraction to assemble the lateral hippocampal network? To test this, we performed an *in vitro* cell aggregation assay using non-adhesive K562 cells. We confirmed that Ten3-expressing K562 cells formed aggregates as previously reported (9), but found that Lphn2-expressing cells did not (fig. S7A and B). However, Ten3-expressing cells aggregated with Lphn2-expressing cells (fig. S7A and B), consistent with the previously reported heterophilic interaction between Teneurins and Latrophilins (10–15). The heterophilic interaction of Ten3 and Lphn2 combined with their complementary expression in the medial versus lateral hippocampal network suggests that the interaction between Lphn2 and Ten3 may result in repulsion, which could allow distinct target selection of axons in the medial and lateral hippocampal networks.

The CA1→subiculum projection develops postnatally (9), therefore we injected lentivirus expressing *GFP* (control) or *GFP-P2A-Lphn2* into the Lphn2-low distal subiculum of mice at P0 to create a region of subiculum expressing Lphn2 across the entire proximal–distal axis. We then injected adeno-associated virus expressing membrane-bound mCherry (*AAV-mCh*) into proximal CA1 in these same mice as adults to label and trace Ten3+ CA1 axons (Fig. 2A, B). The portion of the subiculum transduced by lentivirus was only a subset of the total proximal CA1 axon targeting region along the orthogonal medial–lateral axis, allowing us to determine if proximal CA1 axons target lentivirus-transduced subiculum regions differently compared to neighboring non-lentivirus-transduced subiculum regions.

To visualize the relationship between Ten3+ axon projections and ectopically expressed GFP-Lphn2 in subiculum, we plotted signal intensity from proximal CA1 axons (mCh) and lentivirus injection site (GFP) on the same subiculum graph as color and height, respectively. Expression of GFP alone did not affect the intensity of proximal CA1 axons in the subiculum target (Fig. 2C and fig. S8A–C). However, proximal CA1 axon intensity was reduced in distal subiculum regions ectopically expressing Lphn2 (Fig. 2D and fig. S8D–F; quantified in Fig. 2G). These data suggest that Ten3+ axons are repelled by ectopically expressed Lphn2 at the distal subiculum target.

Repulsion requires Lphn2/Teneurin but not Lphn2/FLRT interaction

To test whether Lphn2-mediated repulsion requires Lphn2/Ten3 interaction, we utilized a deletion of the lectin binding domain in Latrophilins, which has been shown to abolish Teneurin binding without affecting cell-surface expression or interactions with other known partners (12–15). We validated in our K562 cell aggregation assay that Lphn2_ΔLec disrupted Ten3 interaction without affecting interaction with FLRT2 (fig. S7C and D), a member of the fibronectin leucine-rich transmembrane protein family known to bind Latrophilins (11, 17). We then ectopically expressed Lphn2_ΔLec in subiculum to determine if proximal CA1 axon avoidance depends on a Lphn2/Teneurin interaction. We found that in brains ectopically expressing *GFP-P2A-Lphn2_ΔLec*, Ten3+ proximal CA1 axons no longer avoided Lphn2_ΔLec expression regions in distal subiculum (Fig. 2E and fig. S9A–C; quantified in Fig. 2G).

FLRTs interact with Teneurin and Latrophilin to direct synapse specificity and repulsive guidance for migrating neurons (14, 15). Expression of *Flrt2* was enriched in Ten3-high CA1 cells (fig. S3D), suggesting that it may play a role in the repulsion of proximal CA1 axons by target-derived Lphn2. Mutation of four residues in the olfactomedin domain of Latrophilin to alanines abolishes FLRT-Lphn binding while maintaining cell-surface expression and Teneurin binding (18). We confirmed that in K562 cells, Lphn2_4A disrupted FLRT2 binding without affecting Ten3 binding (fig. S7E and F). Yet, ectopic expression of Lphn2_4A in subiculum caused a decrease of Ten3+ proximal CA1 axon intensity in GFP+ distal subiculum regions compared to adjacent GFP– regions (Fig. 2F and fig. S9D–F) to the same extent as wild-type Lphn2 (Fig. 2G). These gain-of-function experiments suggest that repulsion of Ten3+ proximal CA1 axons by target-derived Lphn2 requires Lphn2/Teneurin but not Lphn2/FLRT interaction.

Ten3+ CA1 axons invade *Lphn2*-null subiculum targets

To determine if endogenous *Lphn2* in subiculum is necessary for correct proximal CA1→distal subiculum targeting, we performed a loss-of-function experiment by injecting lentivirus expressing *GFP-Cre* into subiculum of control and $Lphn2^{fl/fl}$ mice (16) at P0, followed by *AAV-mCh* in proximal CA1 of the same mice as adults to assess Ten3+ axon targeting (Fig. 3A and C). In $Lphn2^{+/+}$ control mice, proximal CA1 axons targeted distal subiculum and were not disrupted when projecting into GFP-Cre+ expressing regions (Fig. 3B). By contrast, proximal CA1 axons targeted more broadly in GFP-Cre+ regions in $Lphn2^{fl/fl}$ mice (Fig. 3D). Quantification of proximal CA1 axon intensity in GFP-Cre+ sections revealed that proximal CA1 axons in $Lphn2^{fl/fl}$ mice had increased intensity in the more proximal regions and decreased intensity in the most distal region of the subiculum compared to $Lphn2^{+/+}$ mice (Fig. 3G and H; red vs black). These data suggest that Lphn2 in proximal subiculum normally repels Ten3+ proximal CA1 axons, enabling them to specifically target distal subiculum.

To rule out the possibility that the ectopic invasion of proximal CA1 axons into $Lphn2^{-/-}$ proximal subiculum results from loss of Lphn2 interaction with a molecule other than Ten3 [e.g., another Teneurin that is expressed in CA1 (fig. S3B)], we performed the same *Lphn2*

loss-of-function experiment in *Ten3*$^{-/-}$ mice. Anterograde tracing from proximal CA1 in *Lphn2*$^{+/+}$;*Ten3*$^{-/-}$ mice showed that proximal CA1 axons spread more along the proximal–distal axis of the subiculum (fig. S10A and B). In *Lphn2*$^{fl/fl}$;*Ten3*$^{-/-}$ mice, proximal CA1 axons also showed similar spreading (fig. S10C and D; quantified in fig. S10E and F). The lack of an additional axon mistargeting phenotype in *Lphn2*$^{fl/fl}$;*Ten3*$^{-/-}$ mice compared to *Lphn2*$^{+/+}$;*Ten3*$^{-/-}$ mice suggests that Ten3 is required for the effect of loss of subiculum Lphn2 on proximal CA1 axon targeting, and that Lphn2/Ten3-mediated repulsion instructs proximal CA1→distal subiculum target selection.

Lphn2/Ten3-mediated repulsion and Ten3/Ten3-mediated attraction cooperate

Loss of Lphn2/Ten3 heterophilic repulsion (above) or Ten3 homophilic attraction (9) alone both disrupt precise proximal CA1→distal subiculum axon targeting. What is the relative contribution of each? To address this, we simultaneously conditionally deleted both *Lphn2* and *Ten3* in subiculum and assessed the targeting of Ten3+ proximal CA1 axons (Fig. 3E). We found that proximal CA1 axons projecting into GFP-Cre+ regions of *Lphn2*$^{fl/fl}$;*Ten3*$^{fl/fl}$ mice targeted more proximal regions of the subiculum and also had decreased fluorescence intensity in distal subiculum (Fig. 3F).

Quantification of proximal CA1 axons in GFP-Cre+ subiculum sections of *Lphn2*$^{fl/fl}$;*Ten3*$^{fl/fl}$ mice showed a significant increase in axon intensity into the *Lphn2*$^{-/-}$ proximal subiculum compared to *Lphn2*$^{+/+}$;*Ten3*$^{+/+}$ mice (Fig. 3G and H; blue vs black), confirming a loss of repulsion of Ten3+ proximal CA1 axons from proximal subiculum that normally expresses Lphn2. Additionally, proximal CA1 axons in *Lphn2*$^{fl/fl}$;*Ten3*$^{fl/fl}$ mice had decreased fluorescence intensity in distal subiculum compared to *Lphn2*$^{fl/fl}$;*Ten3*$^{+/+}$ mice (Fig. 3G and H; blue vs red), indicating a loss of attraction of Ten3+ proximal CA1 axons to distal subiculum that normally expresses Ten3. Thus, Lphn2/Ten3-mediated heterophilic repulsion and Ten3/Ten3-mediated homophilic attraction cooperate in orchestrating the precise targeting of proximal CA1 axons to distal subiculum.

Subiculum Ten3 repels Lphn2+ CA1 axons

In addition to serving as a repulsive ligand for target selection of Ten3+ medial hippocampal network neurons, could Lphn2 also act as a receptor to regulate target selection of lateral hippocampal network neurons? Could Lphn2+ axons be repelled from Ten3+ targets to regulate the precision of lateral hippocampal network connections? To test this, we injected lentivirus expressing *GFP-Cre* into subiculum of *Ten3*$^{+/+}$ (control) and *Ten3*$^{fl/fl}$ mice at P0, followed by *AAV-mCh* in mid-CA1 of the same mice as adults to assess Lphn2+ mid-CA1 axon targeting (Fig. 4A and C). In *Ten3*$^{+/+}$ mice, mid-CA1 axons predominantly targeted mid-subiculum (Fig. 4B). However, in *Ten3*$^{fl/fl}$ mice, mid-CA1 axons spread into *Ten3*-null distal subiculum (Fig. 4D). Quantification of axons in subiculum showed a significant increase in axon intensity in distal subiculum of *Ten3*$^{fl/fl}$ mice compared to *Ten3*$^{+/+}$mice (Fig. 4E and F). Thus, Ten3 in distal subiculum prevents Lphn2+ mid-CA1 axon invasion into distal subiculum.

To test if Lphn2 in mid-CA1 axons is required for their target precision, we deleted *Lphn2* from CA1 followed by tracing of *Lphn2*-null mid-CA1 axons (Fig. 4G and I). Control mid-CA1 axons targeted mid-subiculum (Fig. 4H), whereas *Lphn2*-null mid-CA1 axons spread into the most distal subiculum (Fig. 4J, quantified in Fig. 4K and L). Thus, Lphn2 is cell-autonomously required in mid-CA1 neurons to prevent their axons from invading Ten3+ distal subiculum. Taken together with the *Ten3* conditional deletion in subiculum above, these data indicate that Lphn2+ mid-CA1 axons are repelled by target-derived Ten3.

Discussion

Here, we use CA1→subiculum axon targeting as a model to investigate how parallel networks are assembled during development. Our results demonstrate that Lphn2 and Ten3 instruct the precise assembly of both medial and lateral hippocampal networks (Fig. 5A). In the medial network, Lphn2/Ten3-mediated heterophilic repulsion and Ten3/Ten3-mediated homophilic attraction cooperate to instruct proximal CA1→distal subiculum axon targeting; in the lateral network, Ten3/Lphn2-mediated heterophilic repulsion confines Lphn2+ axons to the Lphn2+ target region (Fig. 5B). Additional cell-surface molecules may further subdivide the Lphn2+ region to determine targeting specificity between mid-CA1→mid-subiculum and distal CA1→proximal subiculum. Together, these data indicate that the mechanisms required for parallel network assembly in the hippocampus are intertwined, utilizing multiple interactions of two cell-surface molecules and reciprocal repulsions to ensure the precise segregation of connections.

Our results reveal that Lphn2 acts both cell non-autonomously in targets and cell autonomously in axons during the target selection stage of hippocampal circuit assembly, preceding synapse formation. This is in contrast to previous studies suggesting that Latrophilins act strictly as postsynaptic adhesion molecules to establish or maintain synaptic connections (14, 16, 19). Although defects in axon targeting may contribute to synaptic deficits in *Latrophilin* early postnatal loss-of-function experiments (14, 16, 20), our study is compatible with Latrophilin/Teneurin interactions playing additional roles in synaptic adhesion if the repulsive mechanism is switched off after target selection is complete. While the most parsimonious interpretation is the interactions between Lphn2 and Ten3 mediate repulsion directly, our study does not rule out the possibility that Lphn2/Ten3 interactions initiate signaling cascades that activate repulsive interactions mediated by additional molecules. Latrophilins bind both Teneurins and FLRTs, and the cooperative binding of these three proteins has been implicated in directing synapse specificity and repulsion-mediated neuronal migration (14, 15). However, ectopic expression of a mutant Lphn2 that cannot bind FLRT (fig. S7E and F) still repelled Ten3+ proximal CA1 axons to the same extent (Fig. 2G), suggesting that FLRT binding is not required for Lphn2/Ten3-mediated repulsion during target selection of axons.

Cooperation of attraction and repulsion has been described in neuronal circuit assembly (21, 22). For example, the PlexB receptor interacts with Sema2a and Sema2b through repulsion and attraction, respectively, to mediate axon guidance during *Drosophila* sensory circuit assembly (23). We found that target selection of proximal CA1 axons is determined by Lphn2/Ten3-mediated repulsion from proximal subiculum and Ten3/Ten3-mediated

attraction to distal subiculum (Fig. 3). Thus, Ten3 acts as a receptor for both repulsive and attractive ligands in the same axon during target selection. Conversely, as a ligand, Ten3 acts as an attractant for Ten3+ axons, but a repellent for Lphn2+ axons (Fig. 5).

We show the complementary expression of Ten3 and Lphn2 across all interconnected regions of the hippocampal network. This is reminiscent of Ephrin-A/EphA counter-gradients found across interconnected regions of the developing visual system (24) that utilize bi-directional Ephrin-A/EphA interactions for the formation of topographic projections (25, 26). The patterns of Ten3 and Lphn2 expression across the hippocampal network follow a 'Ten3→Ten3, Lphn2→Lphn2' rule (fig. S4F). The reciprocal repulsions we demonstrated in the CA1→subiculum projection may guide target selection across additional projections to and from the entorhinal cortex. With repeated use in various connections combined with multifunctionality, in which a single protein serves both as receptor and ligand, a limited number of cell-surface molecules can specify a diversity of connections in the mammalian brain.

Supplementary Material

Refer to Web version on PubMed Central for supplementary material.

Acknowledgements:

We thank T. Südhof for the *Lphn2*^{mVenus} and *Lphn2*^{fl} mice, the Neuroscience Gene Vector and Virus Core at Stanford University for producing viruses, D. Berns for advice, inspiration, and artwork, J. Ferguson for artwork, J. Kebschull for MATLAB code, H. Meng for virus preparation, members of the Luo lab for advice and support, D. Berns, J. Kebschull, A. Khalaj, H. Li, J. Li, T. Li, C. McLaughlin, K. Shen and A. Shuster for critiques of the manuscript.

Funding:

D.T.P. was supported by an American Australian Association Education Fund Scholarship. J.H.L. is supported by a National Institutes of Health grant (K01-MH114022). L.L. is an investigator of Howard Hughes Medical Institute. This work was supported by National Institutes of Health grant (R01-NS050580 to L.L.).

Data and materials availability:

The sequencing datasets generated in this study are available in the NCBI Gene Expression Omnibus under accession GSE162552. Custom analysis codes are available at https://github.com/dpederick/Reciprocal-repulsions-instruct-the-precise-assembly-of-parallel-hippocampal-networks. All other data are available in the main paper and supplementary materials. All materials are available through requests to the corresponding author.

References and Notes:

1. O'Keefe J, Dostrovsky J, Brain Res. 34, 171–175 (1971). [PubMed: 5124915]
2. Scoville WB, Milner B, Neuropsychiatry Clin J. Neurosci. 12, 103–113 (2000).
3. Squire LR, Stark CEL, Clark RE, Annu. Rev. Neurosci 27, 279–306 (2004). [PubMed: 15217334]
4. Hafting T, Fyhn M, Molden S, Moser M-B, Moser EI, Nature 436, 801–806 (2005). [PubMed: 15965463]

5. Igarashi KM, Ito HT, Moser EI, Moser M-B, FEBS Lett. 588, 2470–2476 (2014). [PubMed: 24911200]
6. Cembrowski MS et al., Cell 173, 1280–1292.e18 (2018). [PubMed: 29681453]
7. Naber PA, Lopes da Silva FH, Witter MP, Hippocampus 11, 99–104 (2001). [PubMed: 11345131]
8. Tamamaki N, Nojyo Y, J. Comp. Neurol 353, 379–390 (1995). [PubMed: 7538515]
9. Berns DS, DeNardo LA, Pederick DT, Luo L, Nature 554, 328–333 (2018). [PubMed: 29414938]
10. Silva J-P et al., Proc. Natl. Acad. Sci. U. S. A. 108, 12113–12118 (2011). [PubMed: 21724987]
11. O'Sullivan ML et al., Neuron 73, 903–910 (2012). [PubMed: 22405201]
12. Boucard AA, Maxeiner S, Südhof TC, J. Biol. Chem. 289, 387–402 (2014). [PubMed: 24273166]
13. Li J et al., Cell 173, 735–748.e15 (2018). [PubMed: 29677516]
14. Sando R, Jiang X, Südhof TC, Science 363, eaav7969 (2019). [PubMed: 30792275]
15. Del Toro D et al., Cell 180, 323–339.e19 (2020). [PubMed: 31928845]
16. Anderson GR et al., J. Cell Biol. 216, 3831–3846 (2017). [PubMed: 28972101]
17. Jackson VA et al., Structure 23, 774–781 (2015). [PubMed: 25728924]
18. Lu YC et al., Structure 23, 1678–1691 (2015). [PubMed: 26235030]
19. Südhof TC, Neuron 100, 276–293 (2018). [PubMed: 30359597]
20. Sando R, Südhof TC, eLife 10, e65717 (2021). [PubMed: 33646123]
21. Kolodkin AL, Tessier-Lavigne M, Cold Spring Harb. Perspect. Biol. 3 (2011).
22. Sanes JR, Zipursky SL, Cell 181, 536–556 (2020). [PubMed: 32359437]
23. Wu Z et al., Neuron 70, 281–298 (2011). [PubMed: 21521614]
24. Lambot M-A, Depasse F, Noel J-C, Vanderhaeghen P, J. Neurosci 25, 7232–7237 (2005). [PubMed: 16079405]
25. Cang J, Feldheim DA, Annu. Rev. Neurosci. 36, 51–77 (2013). [PubMed: 23642132]
26. Egea J, Klein R, Trends Cell Biol. 17, 230–238 (2007). [PubMed: 17420126]

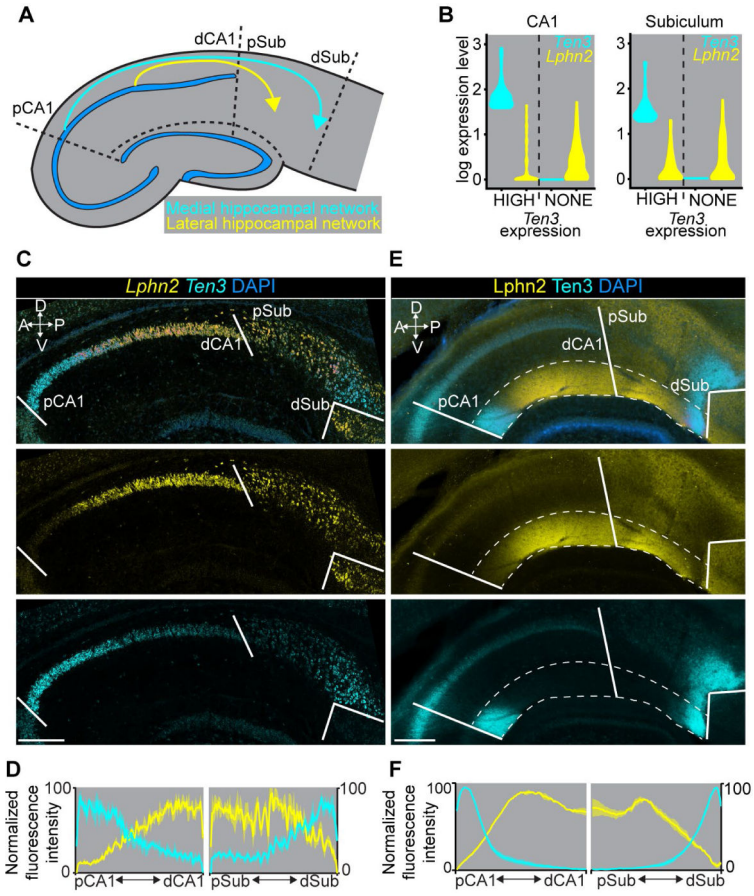

Fig. 1. Complementary expression patterns of Lphn2 and Ten3 in the hippocampal network.

(**A**) Summary of connection patterns of medial (cyan) and lateral (yellow) hippocampal networks. pCA1 and dCA1, proximal and distal CA1; pSub and dSub, proximal and distal subiculum. (**B**) Violin plots highlighting *Lphn2* and *Ten3* expression in *Ten3*-HIGH and *Ten3*-NONE cells in CA1 and subiculum. The unit of expression level is ln [1+ (reads per 10000 transcripts)]. (**C**) Double *in situ* hybridization for *Lphn2* (middle) and *Ten3* (bottom) mRNA on a sagittal section of P8 mouse brain. Solid lines represent boundaries between CA1 and subiculum as labeled in the overlay (top). (**D**) Quantification of *Lphn2* and *Ten3* mRNA across the proximal–distal axis of CA1 and subiculum cell body layers (n = 3 mice). Mean ± SEM. (**E**) Double immunostaining for Lphn2 (middle; anti-GFP antibody) and Ten3 (bottom) on a sagittal section of P8 *Lphn2-mVenus* knock-in mouse (16) brain. Solid lines represent boundaries between CA1 and subiculum as labeled in the overlay (top). Region between dashed lines is the molecular layer. (**F**) Quantification of Lphn2 and Ten3 protein across the proximal–distal axis of molecular layers of CA1 and subiculum (n = 3 mice). Mean ± SEM. Scale bars, 200 μm. Axis labels in this and all subsequent figures: A, anterior; P, posterior; D, dorsal; V, ventral.

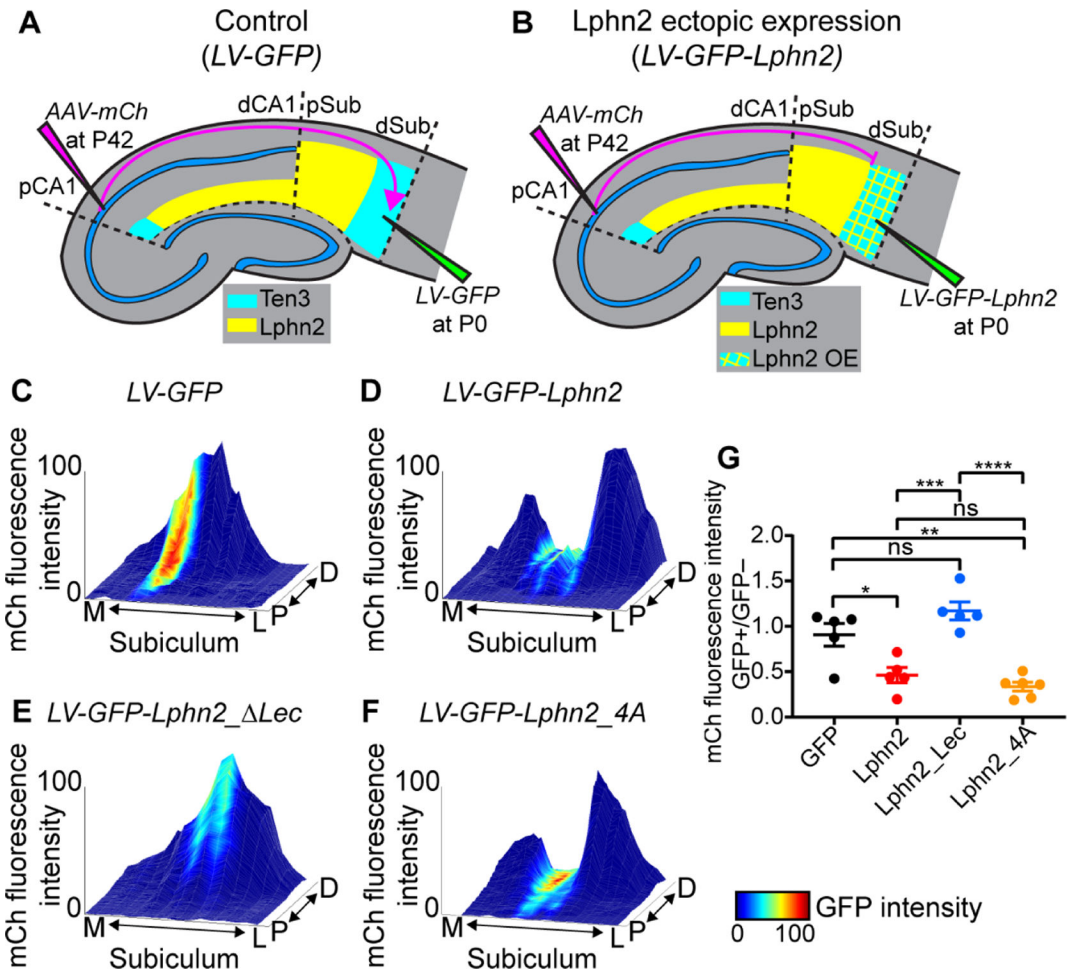

Fig. 2. Ten3+ proximal CA1 axons avoid distal subiculum ectopically expressing Lphn2 in a Lphn2/Teneurin interaction–dependent and Lphn2/FLRT interaction–independent manner.

(**A, B**) Experimental design and summary of results. LV, lentivirus; *AAV-mCh*, adeno-associated virus expressing membrane-bound mCherry as an anterograde tracer. (**C–F**) Representative mountain-plots showing normalized GFP fluorescence intensity as color (LV expression) and normalized mCh fluorescence intensity as height (proximal CA1 axon projections) in subiculum. P, proximal; D, distal; M, medial; L, lateral. (**G**) Ratio of mCh fluorescent intensity of GFP+ versus GFP– regions. *LV-GFP* (n = 5 mice), *LV-GFP-P2A-Lphn2* (wild-type Lphn2; n = 5 mice), *LV-GFP-P2A-Lphn2_ΔLec* (Lphn2 that does not bind Teneurins; n = 5 mice) and *LV-GFP-P2A-Lphn2_4A* (Lphn2 that does not bind FLRTs; n = 6 mice). Mean ± SEM; one-way ANOVA with Tukey's multiple comparisons test. **** $P \leq 0.0001$; *** $P \leq 0.001$; ** $P \leq 0.01$; * $P \leq 0.05$; ns, not significant.

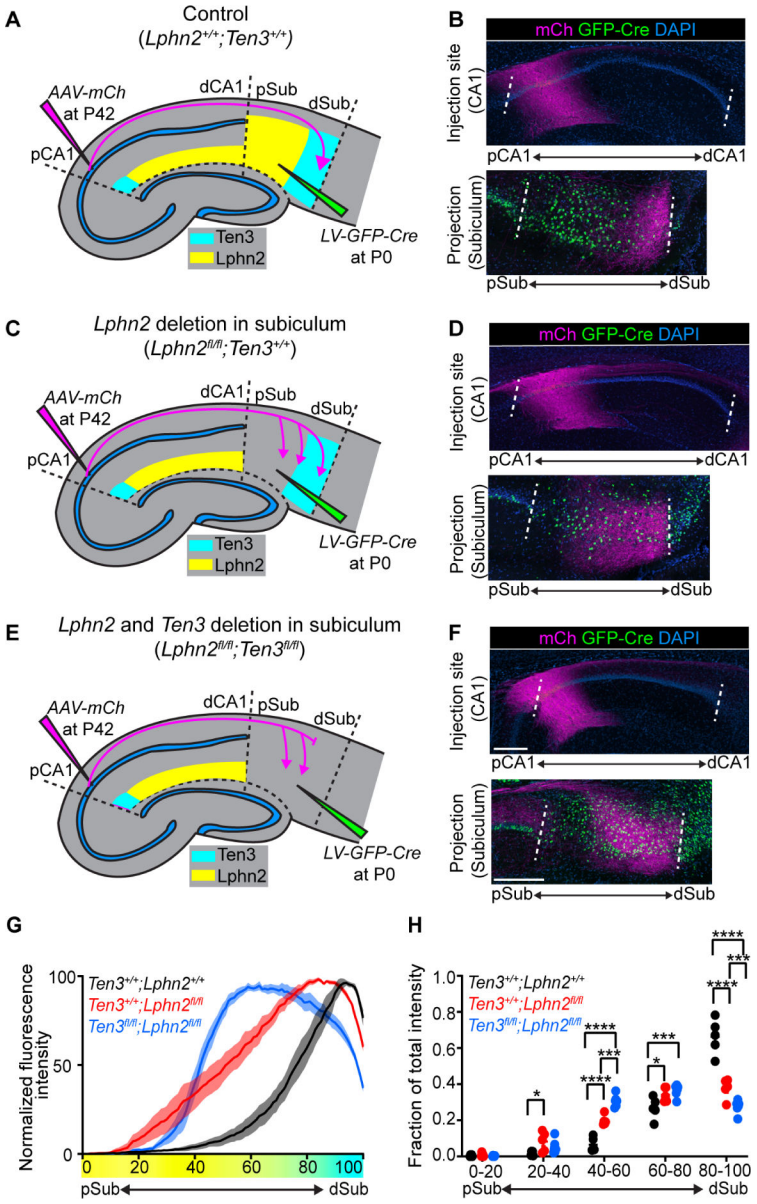

Fig. 3. Lphn2/Ten3-mediated repulsion and Ten3/Ten3-mediated attraction cooperate to guide proximal CA1→distal subiculum target selection.

(A, C, E) Experimental design and summary of results for control (A), *Lphn2* conditional knockout in subiculum (C), and *Lphn2* and *Ten3* double conditional knockout in subiculum (E). (**B**, **D, F**) Representative images of *AAV-mCh* (magenta) injections in proximal CA1 (top) and corresponding projections of proximal CA1 axons overlapping with *LV-GFP-Cre* (green) injection sites in subiculum (bottom). Data in (B), (D), and (F) correspond to experimental conditions in (A), (C), and (E), respectively. (**G**) Normalized mean fluorescence intensity traces of subiculum projections from proximal CA1 in GFP-Cre+ sections for $Lphn2^{+/+};Ten3^{+/+}$ (n = 5 mice), $Lphn2^{fl/fl};Ten3^{+/+}$ (n = 5 mice) and $Lphn2^{fl/fl};Ten3^{fl/fl}$ (n = 6 mice). Mean ± SEM. Color bar under x-axis represents Lphn2 (yellow) and Ten3 (cyan) expression in subiculum as quantified in Fig. 1F. (**H**) Fraction

of total axon intensity for the same data as (G) across 20 percent intervals. Mean ± SEM, two-way ANOVA with Sidak's multiple comparisons test. **** $P \leq 0.0001$; *** $P \leq 0.001$; * $P \leq 0.05$. Scale bar, 200 μm. Injection site locations in CA1 are shown in fig. S11.

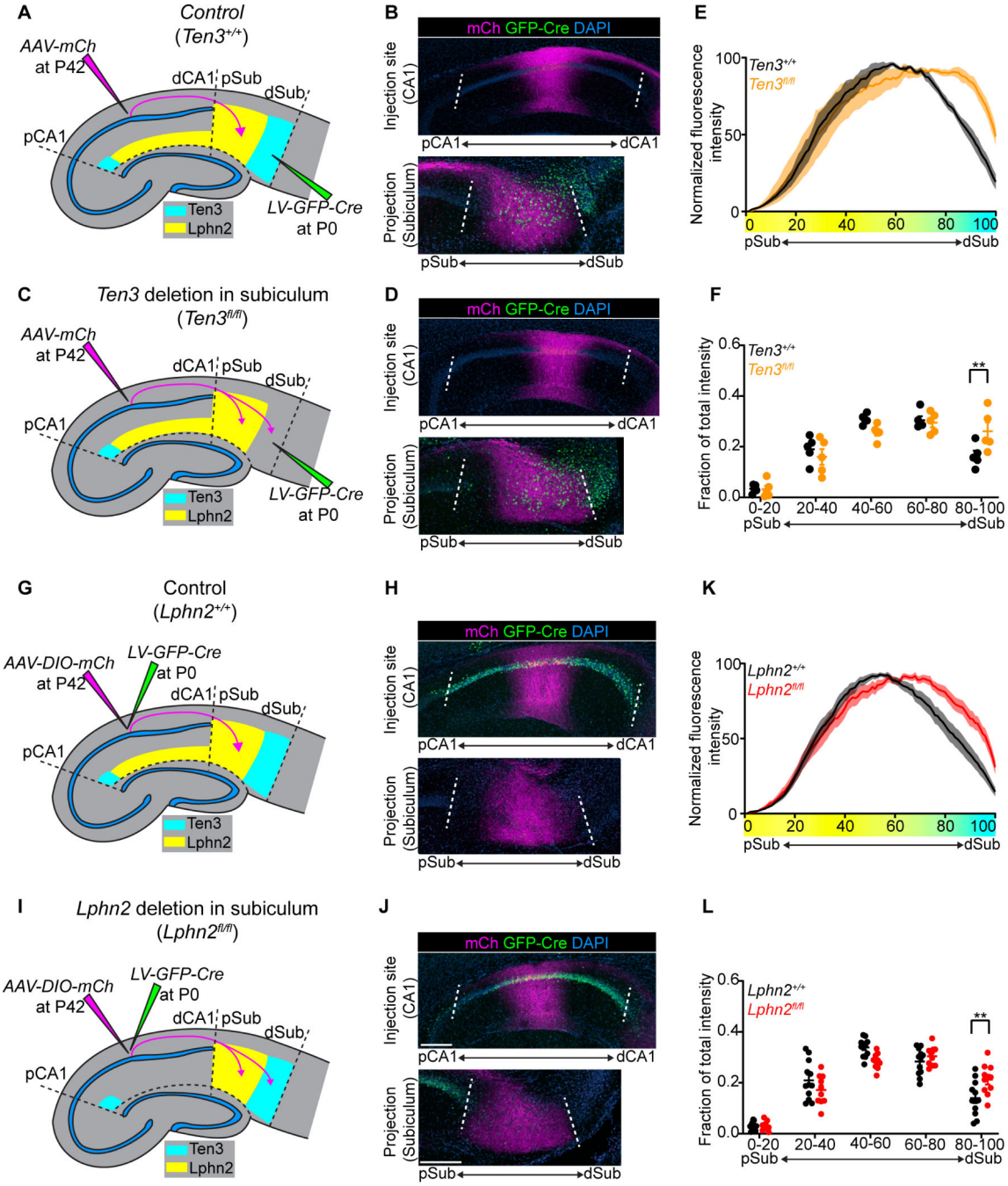

Fig. 4. Lphn2+ mid-CA1 axons avoid Ten3+ distal subiculum.

(**A, C**) Experimental design and summary of results for tracing mid-CA1 axons in control (A) and *Ten3* cKO in subiculum (C). (**B**, **D**) Representative images of *AAV-mCh* (magenta) injections in mid-CA1 (top) and corresponding projections overlapping with *LV-GFP-Cre* (green) injection sites in subiculum (bottom). Data in (B) and (D) correspond to experimental conditions in (A) and (C), respectively. (**E**) Normalized mean fluorescence intensity traces of subiculum projections from mid-CA1 in GFP-Cre+ sections for $Ten3^{+/+}$ (n = 5 mice) and $Ten3^{fl/fl}$ (n = 5 mice). Mean ± SEM. Color bar under x-axis represents

Lphn2 (yellow) and Ten3 (cyan) expression in subiculum as quantified in Fig. 1F. (**F**) Fraction of total axon intensity (same data as E) across 20 percent intervals. Mean ± SEM; two-way ANOVA with Sidak's multiple comparisons test, ** $P \leq 0.01$. (**G, I**) Experimental design and summary of results for tracing control (G) and *Lphn2*-null (I) mid-CA1 axon projections to subiculum. (**H, J**) Representative images of *AAV-DIO-mCh* (magenta; mCh expression in a Cre-dependent manner) injections in mid-CA1 (top) and corresponding projections in subiculum (bottom). Data in (H) and (J) correspond to experimental conditions in (G) and (I), respectively. (**K**) Normalized mean fluorescence intensity traces of subiculum projections from $Lphn2^{+/+}$ (n = 12 mice) and $Lphn2^{fl/fl}$ (n = 10 mice) mid-CA1 axons. Mean ± SEM. Color bar under x-axis represents Lphn2 (yellow) and Ten3 (cyan) expression in subiculum as quantified in Fig. 1F. (**L**) Fraction of total axon intensity (same data as K) across 20 percent intervals. Mean ± SEM; two-way ANOVA with Sidak's multiple comparisons test; ** $P \leq 0.01$. Scale bars, 200 μm. Injection site locations in CA1 are shown in fig. S11.

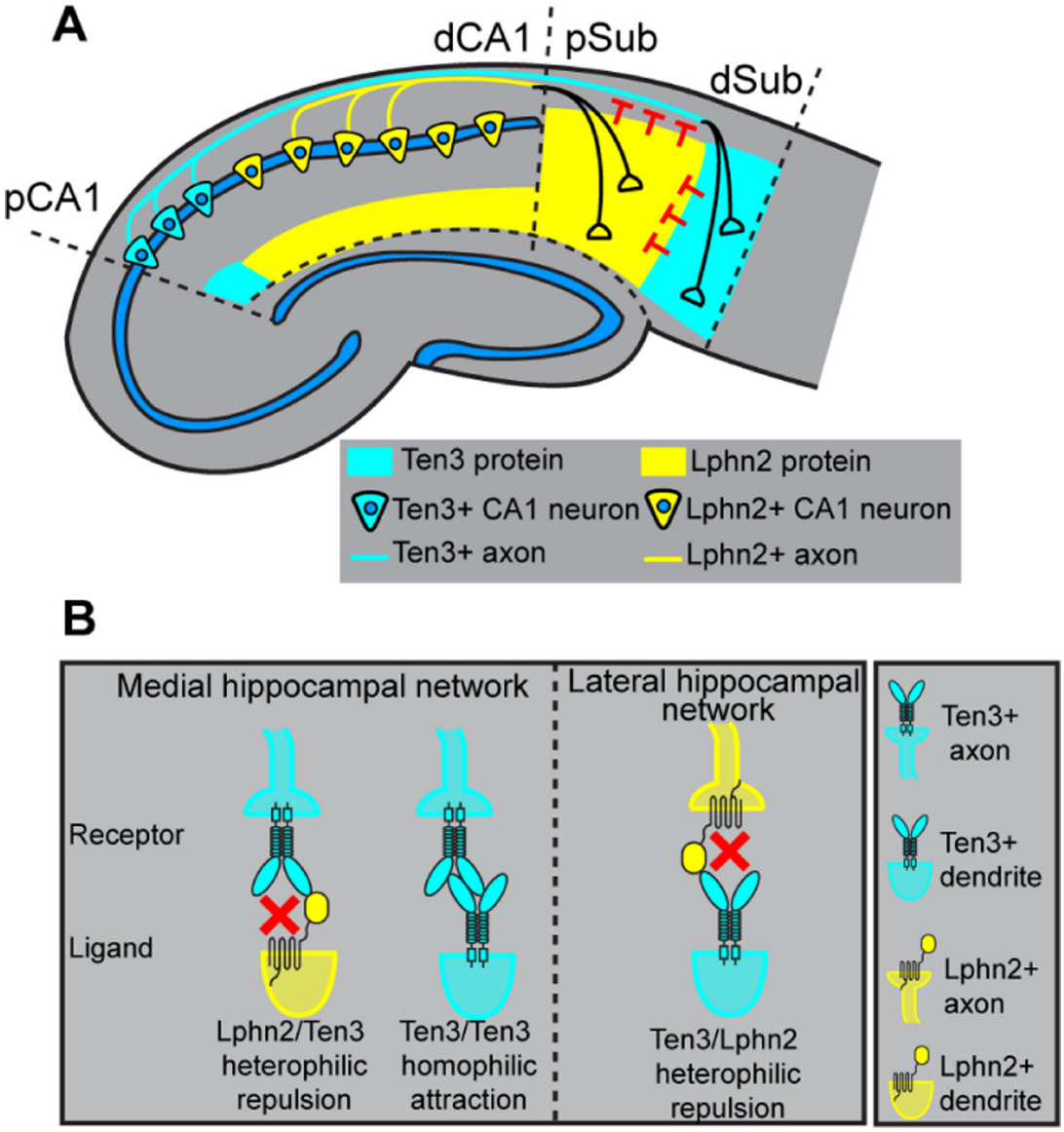

Fig. 5. Lphn2 and Ten3 instruct target selection of hippocampal axons through reciprocal repulsions.

(**A**) Ten3+ CA1 axons target Ten3+ subiculum via repulsion from Lphn2 and attraction to Ten3 in subiculum. Lphn2+ CA1 axons target Lphn2+ subiculum via repulsion from Ten3 in subiculum. (**B**) High-magnification view of ligand–receptor interactions that instruct target selection of Ten3+ (left) and Lphn2+ (right) axons. Red crosses symbolize repulsion.